IEEE Access
Multidisciplinary | Rapid Review | Open Access Journal

Received May 2, 2021, accepted May 24, 2021, date of publication June 2, 2021, date of current version June 11, 2021.

Digital Object Identifier 10.1109/ACCESS.2021.3085307

Omnidirectional Free-Degree Wireless Power Transfer System Based on Magnetic Dipole Coils for Multiple Receivers

CANCAN RONG[1], XIANGRUI HE[1], MINGHAI LIU[1], YUYING WANG[2,3], XIAOBO LIU[1], CONGHUI LU[1], YINGQIN ZENG[1], AND RENZHE LIU[1]

[1]School of Electrical and Electronic Engineering, Huazhong University of Science and Technology (HUST), Wuhan 430074, China
[2]Department of Physics, Xiamen University, Xiamen 361005, China
[3] Jiujiang Research Institute, Xiamen University, Xiamen 361005, China

Corresponding author: Minghai Liu (mhliu@hust.edu.cn)

This work was supported by the National Key Research and Development Program of China under Grant 2018YFB0106300.

ABSTRACT Wireless power transfer (WPT) technology offers a potential solution for the energy-supply problem. In this paper, we propose a novel magnetic coupling mechanism for omnidirectional and multiple-pickup energy transfer based on the magnetic dipole coils. Firstly, a cubic transmitter structure capable of generating three-dimension (3D) homogeneous magnetic field is fabricated to weaken directional sensitivity of receiving coil. Furthermore, the direction of current flowing through each dipole coil is also studied in detail. Numerical and simulated analysis is implemented to verify the omnidirectionality of the transmitter. Secondly, the equivalent circuit model for WPT systems with ferrite is analyzed. In addition, optimal loads, power distribution and transfer efficiency for multiple receivers are discussed and used to achieve the proper system design. Finally, experimental prototype is set up to validate the transmission performance of the proposed WPT system. The results have showed that genuine 3D high degree of freedom (DoF) can be achieved. Meantime, above 60% efficiency at least 30 W of total output power can be obtained for WPT systems with eight pick-ups. We believe the proposed system will give a new guideline for future low power electronic applications, such as monitoring sensors, miniature robots and household devices.

INDEX TERMS Magnetic dipole coil, cubic transmitter, omnidirectional system, multiple pickups, wireless power transfer (WPT).

I. INTRODUCTION

Wireless power transfer (WPT) technology has attracted much attention due to many advantages, such as safety, convenience and reliability. WPT technology via strongly magnetic coupling resonance, introduced by MIT in 2007 [1], is a promising way to charge the electrical equipment. However, the transmission efficiency decreases sharply when the magnetic coupling mechanisms are not aligned very well [2]. In particular, for dynamic and multiple pick-ups charging, it is a critical problem to avoid the adverse impacts caused by misalignment conditions.

In fact, omnidirectional WPT systems have been reported in numerous previous papers, which aimed to be insensitive to the positional misalignment. For most omnidirectional WPT systems, the coupling mechanism design is considered as essential strategy to ensure the uniformity of space magnetic field (MF). According to the coil configurations, omnidirectional WPT systems mainly can be divided into orthogonal coil, stereoscopic structure, magnetic-dipole-based structure and rotational structure.

(1) Orthogonal coil: orthogonal structure is currently the most commonly used in omnidirectional WPT systems due to simple structure and great homogeneity of 3D MF [3]–[13]. Fig. 1 shows the typical structural diagrams of three orthogonal square coils and three orthogonal round coils. Three orthogonal coils are connected to three power supplies to generate a spatially rotating MF, thus achieving 3D omnidirectional wireless charging outside or inside the transmitter. For these coil structures, the non-identical current controls are key considerations, such as current amplitude modulation, phase angle modulation and frequency control. In general,

The associate editor coordinating the review of this manuscript and approving it for publication was Zhehan Yi.

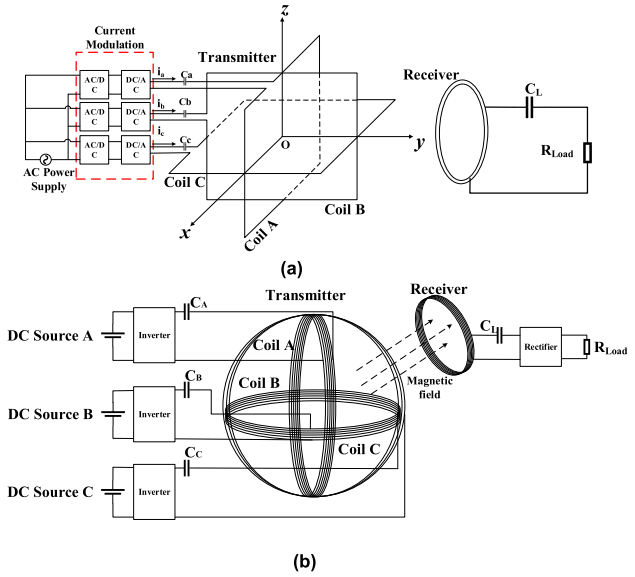

FIGURE 1. Typical orthogonal coil. (a) Three orthogonal square coils. (b) Three orthogonal round coils.

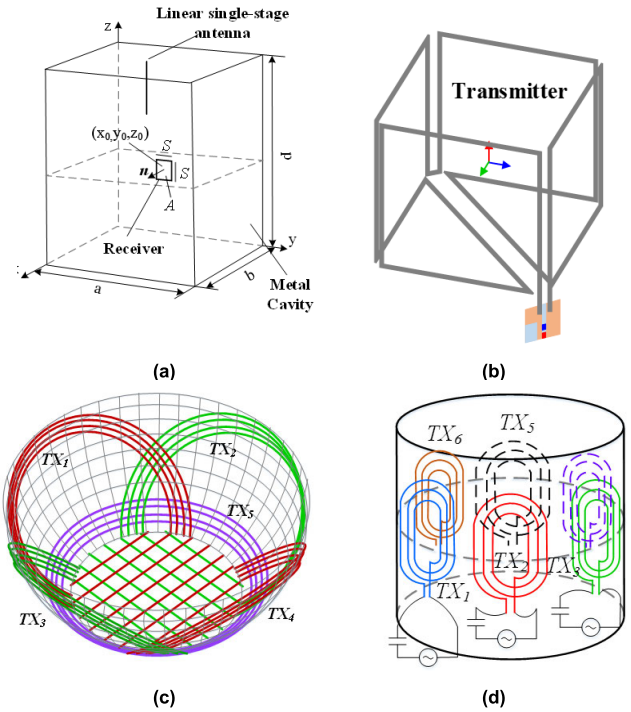

FIGURE 2. Stereoscopic coil. (a) Cavity resonator (b) Cubic coil. (c) Bowl-shaped coil. (d) Cylinder coil.

the load detection technique and feedback control circuit are required, which leads to complex system design and economic consideration. Table 1 lists current control comparisons of main state-of-the-art studies.

(2) Stereoscopic structure: In order to achieve the omnidirectional WPT systems, the special shapes of the stereoscopic coils have been applied [14]–[18], such as cavity resonator, bowl-shape coil, cubic coil and cylindrical coil, as shown in Fig. 2. In [14], hollow metallic structure was proposed to generate homogeneous magnetic field based on electromagnetic cavity resonance. Ha-Van N, Seo C [15] proposed an omnidirectional WPT system with a cubic transmitter to attain great DoF at the relatively high power efficiency. However, the working frequency at 13.56 MHz is too high. Junjie Feng *et al.* [16], [17] proposed a bowl-shaped transmitter to attain strong and uniform omnidirectional magnetic field distribution (MFD) for portable devices. In [18], a number of planar coils are arranged evenly on the sides of the cylinder, the current phase control had been adopted for rotating MF. These coils are suitable for specific situations due to the particularity of the structures.

(3) Magnetic-dipole-based structure: Compared with the air resonance coil, the coil with soft magnetic materials can enhance the magnetic coupling effectively. Hence, the physical dimension of coil structure can be largely reduced in the case of comparability. In addition, ferromagnetic material can guide the magnetic flux where the electromagnetic field is concentrated and eventually cancel the electromagnetic noise around the systems. Ferrite core, which has high relative permeability and low relative conductivity, is widely used in WPT systems due to its availability, stability and practicability [19]–[23]. In [24], the crossed dipole coil was proposed for 3D omnidirectional WPT systems. The rotating MF was generated by the direct and quadrature (DQ) inverter. However, the transfer distance is very small (5 mm). In [25], a uniformly MFD based on magnetic dipole coil was presented and six DoFs are achieved with multiple plane receiving coil (RX) coils. In [26], RX coil of regular tetrahedron structure based on a ferrite core was designed to realize energy charging from an arbitrary angle in 3D space.

(4) Rotational structure: As shown in Fig. 3, the rotational structure consists of one transmitting (TX) coil, which is fixed on the motor rotor and connected with the power supply through an electric slip ring [27]. The motor drives TX coil to rotate at a certain speed, forming the alternating rotating magnetic field in two-dimensional space. The spatial magnetic field distribution can be optimized by adjusting the speed of the motor. Yan *et.al* [28] proposed a rotation-free WPT system achieving stable output power and efficiency under the condition of rotational misalignment.

In a word, transmitter structure design for omnidirectional uniform magnetic field and current modulation are two common methods against misalignment. The majority of these works were based on a 3D omnidirectional MF and one pick-up receiver, which lacks analysis of multi-load situations. Only one RX coil cannot realize the maximum utilization of omnidirectional energy. Moreover, few papers discussed a genuine 3D omnidirectional implementation for arbitrary spatial positions.

For numerous distributed random loads, such as IoT sensors and household applications, the studies for multiple pick-ups are of great significance. In [29], the circuit-model-based analysis was implemented for clustered multi-load receiving (RX) coils. The effects of the mutual inductance and loads for WPT performance were studied in detail. In [30], the WPT systems with multiple transmitters or

TABLE 1. Current control comparison for high-quality articles ('-' means not given).

Reference	Orthogonal structure	Current modulation	Resonant Frequency	Power	Efficiency
[4]	Square	Six variations, amplitude and phase control	19.59 kHz	13.7 W	28.2%
[6]	Round	Three-phase-shifted drive	202 kHz	22.7-62.7	19.1-52.3
[8]	Round	Two variations, amplitude control	535 kHz	-	-
[10]	Round	Weighted time-sharing scheme	-	1.07W	69.5%
[12]	Round	Selective frequency modulation	290kHz/640kHz	-	-

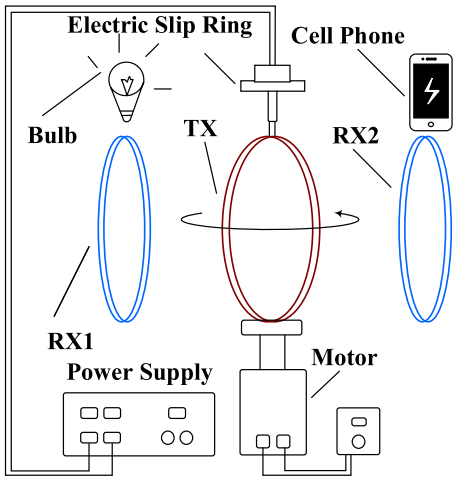

FIGURE 3. Rotational omnidirectional structure.

multiple receivers were discussed. The frequency adjustments in various conditions were investigated for maximum efficiency. Zhen Zhang *et.al* [31] proposed a continuously adjustable capacitor to improve the energy security performance for multiple pick-ups. This method can be used in single-power-induced energy field for WPT systems. In [32], a novel receiver consists of two parallel coils in front of rectifier was designed to adjust the output voltage, which can avoid the occurrence of overvoltage and low voltage.

In general, the RX coil is far smaller than the TX coil for multi-load WPT systems. Then multiple RX coils have more space to move and the free positioning can be naturally guaranteed. For most coil structures mentioned above, especially orthogonal coils, the dimensions of the RX coils are the same as those of the TX coils due to the consideration to maintain greater coupling strength. In addition, the operating frequency is always set up to megahertz for high Q factors, which will lead to extremely narrow resonant frequency bandwidth. The electrical parameters are very sensitive to ambient surroundings at high frequency. Instead of efficient switching converters, the RF power amplifiers will be used, which would reduce the transmission efficiency of the WPT systems. The introduction of the ferrite can reduce the size of RX coil greatly due to strong coupling ability and inherently suitable for multi-load charging. In the meantime, the ferrite exhibits great properties at kHz range, such as high permeability and low permeability, which can enhance the coupling strength between the coils and reduce the eddy-current loss of the ferrite.

In this paper, a 3D WPT systems based on magnetic dipole coil for omnidirectional and multiple-pickup transmission is proposed. In Section II, the optimal design for transmitter coil is investigated in detail, especially for the determination of current direction of each dipole coil. Some other variables, such as turn number of coil and the length of ferrite have been analyzed to optimize the coil structure. In Section III, the equivalent circuit method of the WPT systems with ferrite is discussed. In Section IV, two types of experiments have been implemented to validate the feasibility of the proposed WPT systems. Finally, the conclusion is drawn in Section V. The main contributions of this paper are as follows.

1) The magnetic dipole coil and cubic transmitter structure are combined to realize omnidirectional wireless charging for multiple pick-ups.
2) A genuine 3D omnidirectional characteristic is achieved, rather than just around the transmitter in 2D occasions. In addition, the excitation currents of RX coils in three directions (XOY, YOZ and XOZ) are identical.
3) The proposed WPT systems can simultaneously power up to eight loads in any arrangement. It can provide above 30 W output power and about 60% dc-to-load efficiency.

II. COIL DESIGN

The magnetic resistance of the ferrite core is far smaller than the air and the relative permeability is above 3000. It has been proved that the ferrite can induce the magnetic coupling and guide the trend of magnetic flux [20]. The magnetic intensity can be improved when the coil is inserted with the ferrite. In the WPT coupled systems, the self-inductance and mutual inductance of the coil are key parameters, directly affecting the system performance. Based on the ANSYS Maxwell software, it can be simulated that the inductances of the coil with the ferrite are several hundred times the inductance of coil without the ferrite when the turn numbers of two coils stay the same. As for the magnetic dipole coil, the coupling coefficient varies with the distance before and after adding the magnetic core, as shown in the Fig. 4. It can be seen that the coupling coefficient between the coils with the magnetic core added is dozens of times larger than that without the core added, but both cases generally decrease with the increase of transfer distance. Therefore, the dipole coil can enhance the coupling between resonators greatly.

In the meantime, the self-inductance of the coil and the magnetic density of the core increase with the number of the turns of coil and the length of the core, as shown in Fig. 5. It can be seen that the inductance is positively related to the turn number and length of coil. Moreover, if the length of the magnetic core is fixed and does not exceed the saturated

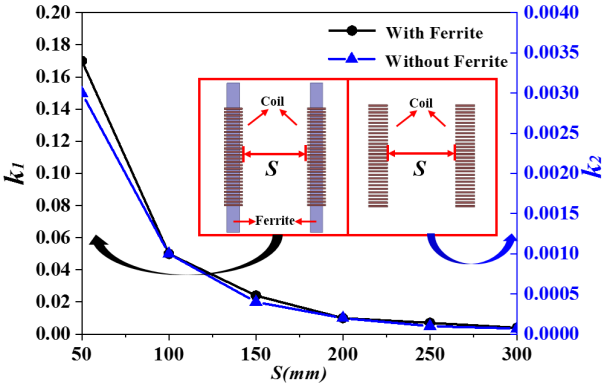

FIGURE 4. The coupling coefficient (k) varies with distances. The left vertical coordinate represents value of the coupling coefficient with the ferrite. The right vertical coordinate represents value of the coupling coefficient without the ferrite.

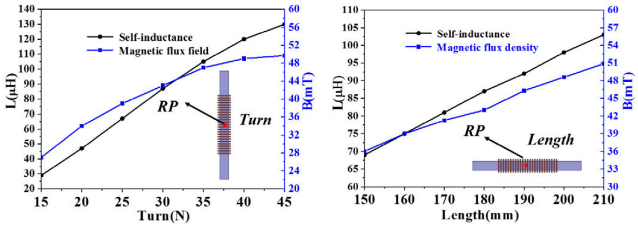

FIGURE 5. Variation diagram of the self-indutance and magnetic induction intensity. (a) Number of coils; (b) Length of the ferrite.

magnetic flux of the ferrite core, the magnetic field gets larger when the turns of the coil increases. Ultimately, after a series of optimization designs and simulation analysis, ferrite core at 180mm × 15mm × 15mm in size and 30 turns are used for magnetic dipole coil in consideration of weight, volume and fabrication of the resonators.

A. CURRENT DIRECTION OF CUBIC TRANSMITTER

In order to obtain stable and high-efficiency omnidirectional WPT system, a cubic transmitter of magnetic dipole coil is designed, as shown in Fig. 6(a). The proposed cubic TX coil consists of 12 magnetic dipole coils and each dipole coil is wound with multiple turns of Litz wire. It is very complicated to establish its physical simulation model in the finite element simulation software according to the actual structure. In order to obtain a high enough simulation accuracy, the mesh needs to be finely divided, and the finite element number of the model is huge, which will be time-consuming, or even the possibility of no solution. Therefore, the geometry of multi-turn coil on each side can be replaced by a single long coil in order to reduce the complexity. It has been proved that this simplicity is feasible and accurate and just for current direction analysis [23], [24]. It is worth noting that the simplified process is not used to obtain the electrical parameters of the coils, but only to gain the direction of each magnetic dipole coil for omnidirectional MFD. According to the magnetic distribution of the dipole coil, the coil can be viewed as the magnetic pole, as shown in Fig. 6(b). The direction of magnetic pole is determined by the current direction of

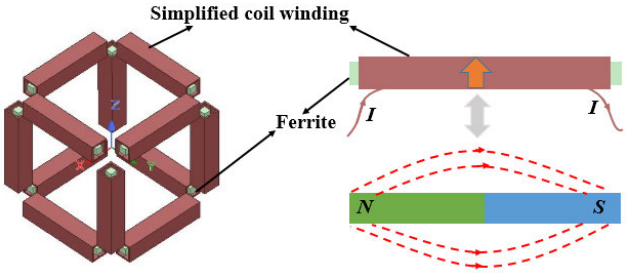

FIGURE 6. The coupling coefficient varies with distance. The left vertical coordinate represnets value of the coupling coefficient with the ferrite. The right vertical coordinate represnets value of the coupling coefficient without the ferrite.

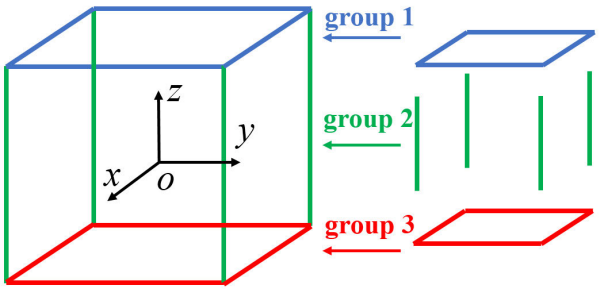

FIGURE 7. Simplified diagram of transmitter coil groups.

the magnetic dipole coil. To achieve the 3D uniformity of the omnidirectional magnetic field, the current directions of 12 dipole coils need further discussion.

Since the transmitter is in series, there are two cases for each dipole coil: 'N-S' type and 'S-N' type. Therefore, there are 2^{12} combined connection modes totally. For better analysis, 12 dipole coils are divided into three groups, as shown in Fig. 7. Assuming all three groups of coils can generate symmetric magnetic field, then the cubic transmitter could achieve omnidirectional magnetic field according to the superposition theorem. Hence, the current direction of dipole coils can be designed in each group separately, which can greatly simplify the analysis process.

Step1-Design the current directions for coils in group 1/3: Since group 1 and 3 are symmetric and share the same structure properties, group 1 is discussed in detail while group 3 is neglected for better declaring the process. There are 2^4 combined connection modes for group 1, as shown in Fig. 8(a). To better illustrate, all cases are signed using "N-S (S-N)" type. In order to achieve symmetric and strong magnetic field, 12 cases are neglected for their asymmetric structure or magnetic field canceling. Hence, the selected four cases can be grouped into one due to the angular-symmetry in the space, as shown in Fig. 8(b). Therefore, the current direction for coils in group 1, as well as group 3, can be determined. Fig. 9 shows the MFDs for three different cases, it can be found that MFD of the first case is symmetry and enhanced around the coil.

Step 2-Analyze and determine the angle between group 1 and 3: Because this structure is symmetric, analysis for one plane is reasonable to identify the major feature of the magnetic field. It can be seen that the magnetic

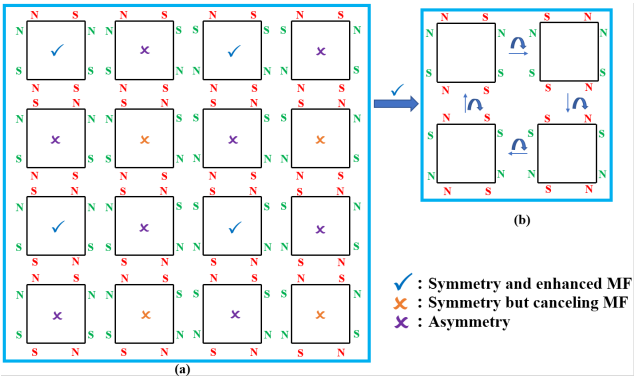

FIGURE 8. The design process for group 1/3. (a) All cases for the connection using 'N-S' type. (b) The angular-symmetry cases for the connection using 'N-S' type.

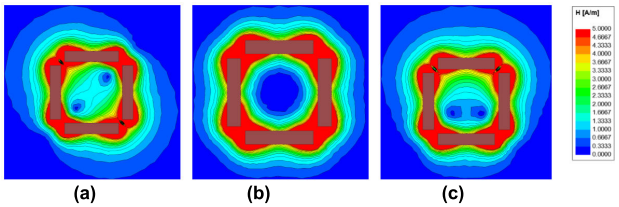

FIGURE 9. Magnetic field distribution for group 1/3. (a)Symmetry and enhanced MF. (b) Symmetry but canceling MF. (c) Asymmetry.

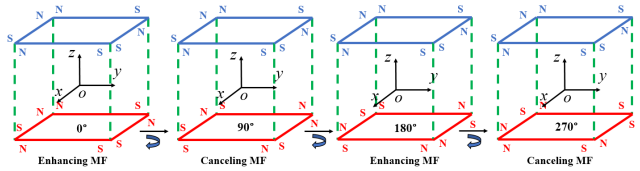

FIGURE 10. All cases for the combination of group 1 and group 3.

field is symmetric but orientated. Hence, the symmetry of magnetic field will be affected by the angle between group 1 and group 3. There are four cases for the combination of group 1 and 3, in other words, the angle is 0°, 90°, 180° and 270°, as shown in Fig. 10. Fig. 11 shows the MFDs of four different cases. Simply, the cases of 90° and 270° can be excluded because the magnetic fields of the surrounding points are weakening or enhancing each other. Considering the directions of the magnetic field, the case of 180° is neglected because the field has been counteracted and asymmetry. Therefore, the 0° case is the only one satisfies symmetry and enhanced magnetic field, which means the angle between group 1 and 3 can be determined.

Step 3- Design the current directions for coils in group 2: there are 2^4 combined connection modes for group 2. However, based on the 3D omnidirectional demands, the whole dipole should satisfy symmetry in the space. Therefore, the transmitter is rotated along x or y axis and repeat *step 1* and *step 2* twice. The result is shown in Fig. 12, with only two results remain.

After permutation and combination, there are only two cases that satisfy the uniformity requirement unrepeatably in the end. Fig. 13 shows two different connection modes and corresponding MFD diagrams. It is worth noting that these graphs only show the MFD in XOY plane. However,

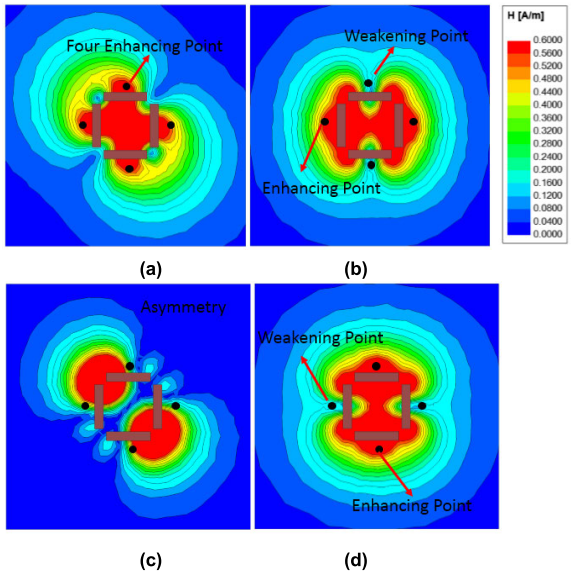

FIGURE 11. Magnetic field distribution. (a) 0°, (b) 90°, (c) 180°, (d) 270°.

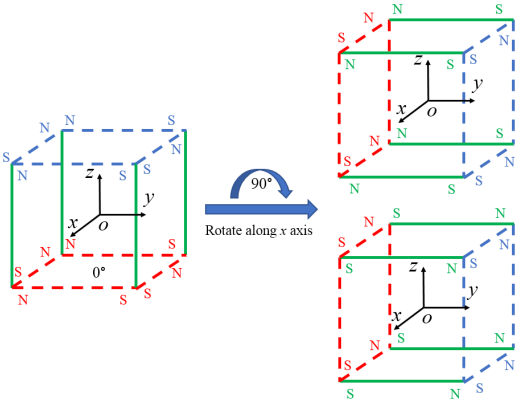

FIGURE 12. The design process for group 2.

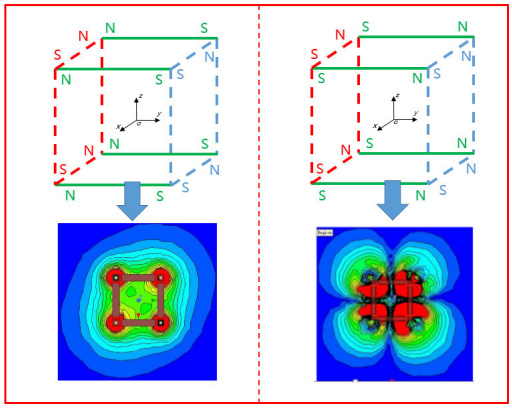

FIGURE 13. Magnetic field distribution of two ways of winding for TX coil.

the MFDs in YOZ and XOZ plane are also same as that in XOY plane, which agrees with the theoretical analysis for omnidirectional transmission. It can be obviously seen that the MFD of the first connections is basically identical. Whereas the second is symmetric, but the magnetic field is very uneven around. For these reasons, the transmitter model

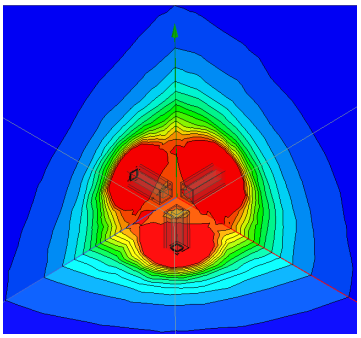

FIGURE 14. 3D Magnetic field distributions for proposed cubic TX coil.

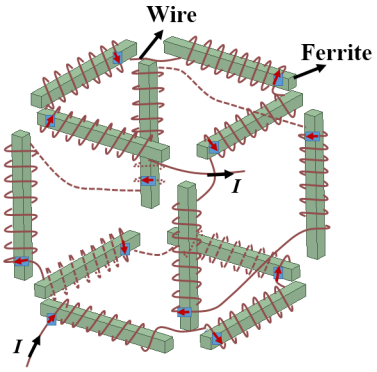

FIGURE 15. Electrical connection among 12 magnetic dipole coils.

of the first connection mode is adopted to optimize the design process.

Fig. 14 shows the 3D MFD diagram of the proposed cubic TX coil. A vertex angle of the cubic coil is selected and it can be seen obviously that the magnetic field is uniformly distributed in all directions. After the above series of analyses, the electrical connection among 12 magnetic dipole coils can be shown as Fig. 15.

To verify the omnidirectional property of the TX coil, the Near Field Probe and Spectrum Analyzer are adopted to measure the magnetic field generated by cubic transmitter coil, as shown in Fig. 16. In this experiment, the magnetic fields of three directions, namely XOY, YOZ, XOZ, are measured firstly, as shown is Fig. 17(a). The magnetic fields are measured with a distance of 30 cm apart from the origin of the coordinate system. The working frequency of the WPT systems is 84.5 kHz, which is designed to meet J2954 (nominal frequency range is 81.38-90 kHz) drafted by the Society of Automotive Engineers task force [20]. The current flowing through the transmitter is set as 2 A. It can be found that there is a great agreement of three curves and indicates the real 3D omnidirectional performance of transmitter coil. Secondly, arbitrarily direction to be measured of the transmitter coil is selected and the position is fixed, while the test point is in turn moved around the transmitter coil at various receiving angles and different distances, as shown in Fig. 17(b). In the case of short distances, the magnetic field values on the diagonal are slightly higher than the points measured directly against the coil. This is because the diagonally magnetic dipole closer to the test point has a larger magnetic field than other dipoles.

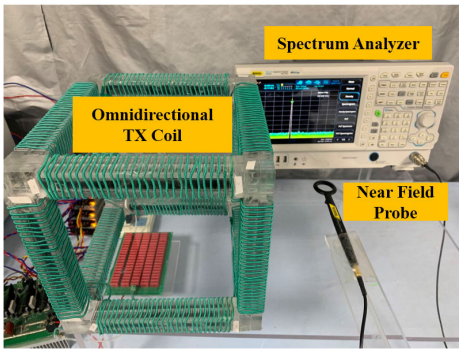

FIGURE 16. Measurement configuration for magnetic field intensity of the TX coil (The AC current is 2A).

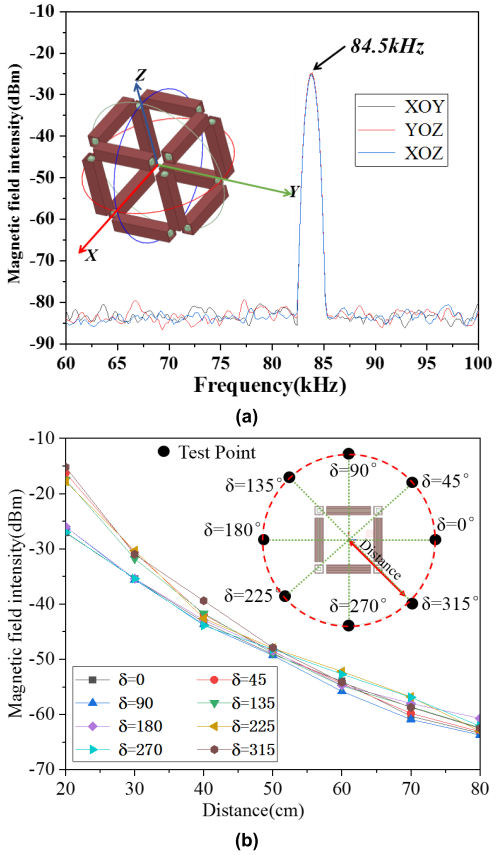

FIGURE 17. Measurement of magnetic field intensity corresponding to (a) Three planes. (b) Receiving angle.

When the distances increase, the influence weakens and the magnetic field is almost the same in all directions.

B. SELECTION OF THE RX COIL

In order to achieve the great coupling strength and reduce the size of RX coil, the magnetic dipole structure is also adopted of RX coil instead of the planar coil. It is assumed that the RX coil is smaller than the TX coil and that the RX coil has enough positioning space due to large uniform magnetic field [24]. The design and control of the 3D RX coil are relatively complicated, there are even cases where the magnetic fields cancel each other out. Therefore, the small 1D RX coil is designed and fabricated in this paper. Fig. 18 shows

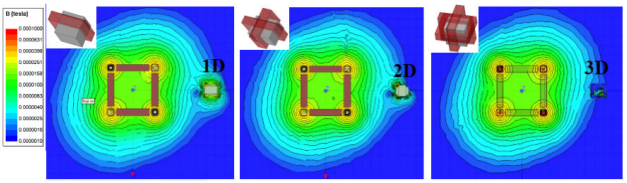

FIGURE 18. Magnetic field distributions for Rx coils of different dimensions.

the MFDs of WPT systems when the Rx coil is wound in 1D, 2D and 3D situations, respectively. It can be seen that the received magnetic field of 1D RX coil is larger than other cases due to the potential magnetic field cancellation.

III. THEORETICAL ANALYSIS FOR PROPOSED WPT SYSTEM

A. MODEL OF THE CIRCUIT THEORY

Fig. 19 depicts a simplified schematic circuit diagram of traditional two-coil WPT systems with air core and the proposed WPT systems. Compared with equivalent circuit of the traditional WPT system, auxiliary circuit parameters (R_f, L_f and C_f) are introduced due to the existence of the ferrite coil. In addition, ΔM denotes the variation in mutual inductance [19].

The power transfer efficiency (PTE) can be expressed for the traditional two-coil WPT systems when the system is tuned in a resonant state as [33]

$$PTE = \frac{R_L}{(R_2 + R_L)(\frac{R_1(R_2+R_L)}{(\omega_0 M_{12})^2} + 1)} \tag{1}$$

where the power supply frequency ω is set to resonant frequency ω_0 and defined as

$$\omega = \omega_0 = \frac{1}{\sqrt{L_1 C_1}} = \frac{1}{\sqrt{L_2 C_2}} \tag{2}$$

Considering the resonator with high quality factor and practical industrial condition of source and load, we assumed that $R_2 \ll R_L$, therefore, $R_2 + R_L \approx R_L$. The efficiency can be simplified as

$$PTE = 1 \Big/ (1 + R_L R_1 \Big/ (\omega_0 M_{12})^2) \tag{3}$$

For the proposed WPT systems with ferrite, the circuit parameters vary when the ferrite core is added in the system. The auxiliary capacitance C_f is introduced mainly because of the existence of parasitic capacitance between the core and wire for the magnetic dipole coil [23]. It should be noted that C_{f1} and C_{f2} can be neglected due to small configuration of magnetic coupling mechanism, compared with C_1' and C_2' [34]. Here, the operating frequency ω keeps constant via tuning the values of compensation capacitors. The resonant frequency ω_0 is also the same to the original value and can be given by

$$\omega = \omega_0 = \frac{1}{\sqrt{(L_1 + L_{f1})C_1'}} = \frac{1}{\sqrt{(L_2 + L_{f2})C_2'}} \tag{4}$$

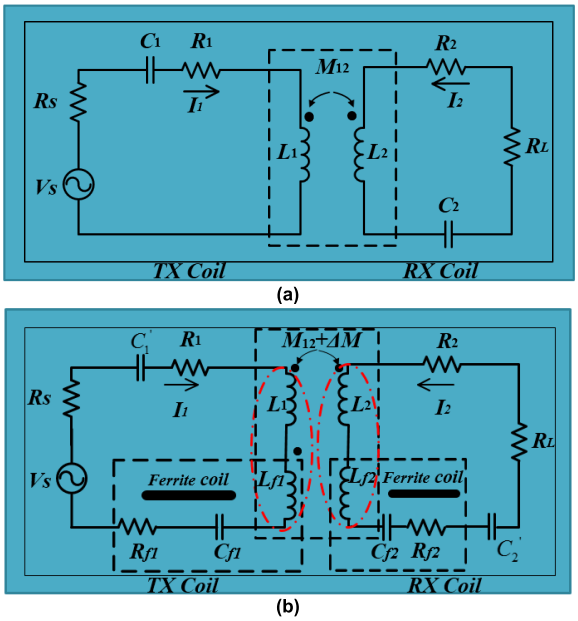

FIGURE 19. Simplified schematic circuit diagram. (a) Traditional two-coil WPT system with air coil. (b) Proposed omnidirectional WPT system with ferrite.

The transfer efficiency can be simplified as

$$PTE' = 1 \Big/ (1 + R_L(R_f + R_1) \Big/ (\omega_0 (M_{12} + \Delta M))^2) \tag{5}$$

According to (3) and (5), the mutual inductance between the coils and parasitic resistances vary when the ferrite coil is introduced in the WPT systems. Accordingly, the transmission efficiency will be changed correspondingly. Here, transfer efficiency ratio (β) is defined to reflect variations in efficiency before and after the addition of ferrite core. It is defined by

$$\beta = PTE'/PTE \approx \frac{1 + \alpha \frac{(R_1 + R_{f1})R_L}{(\omega_0 (M + \Delta M))^2}}{1 + \frac{(R_1 + R_{f1})R_L}{(\omega_0 (M + \Delta M))^2}} \tag{6}$$

where gain factor α is the relation between the inductance and resistance. It can be calculated as

$$\alpha = \frac{(\Delta M/M + 1)^2}{\Delta R_1/R_1 + 1} \tag{7}$$

When $\alpha > 1$, β will be larger than 1. Under this condition, the transmission efficiency would be enhanced. Conversely, the efficiency would be reduced. Based on the simulation analysis mentioned above, the increment of mutual inductance is largely greater than the increment of resistance for magnetic dipole coil, which means that the proposed WPT systems with ferrite can contribute to improve the transmission efficiency.

B. MULTIPLE RX COILS

Fig. 20 shows the equivalent circuit model for multiple-RX WPT systems. AC voltage source with RMS amplitude is defined as VS and the working frequency is denoted as ω. For simplicity, the influences of ferrite for circuit parameters

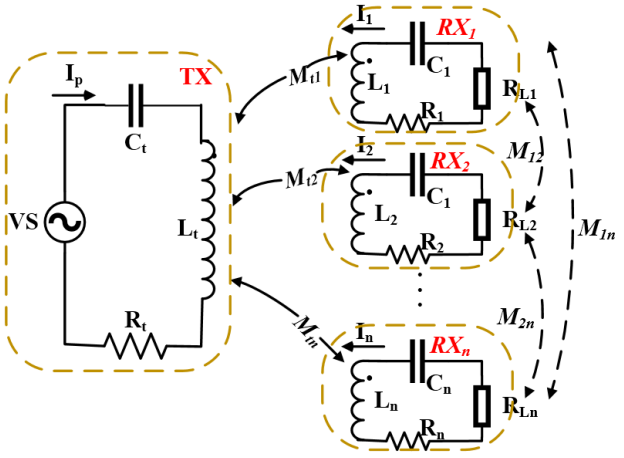

FIGURE 20. Equivalent circuit for multiple-RX WPT system.

have been considered into *RLC* in the Fig. 19. The mutual inductance M_{ti} represents the strength of coupling between the TX coil and each RX coil, and M_{ij} is defined as the mutual inductance between RX coils.

A circuit-model-based numerical theory has been implemented for a single RX coil WPT system. It can be seen that the system transmission performance depends heavily on the coupling and load resistance. To simplify the analysis, the couplings between RX coils are ignored. The reasonableness of this neglect will be proved later. For multiple RX coils, the overall system efficiency can be expressed as [35]

$$PTE = \frac{\sum_{i=1}^{n} Z_{Ri} \frac{R_{Li}}{R_i + R_{Li}}}{(R_t + \sum_{i=1}^{n} Z_{Ri})} \tag{8}$$

Here,

$$Z_{Ri} = \frac{(\omega M_{ti})^2}{R_{Li} + R_i} \tag{9}$$

In general, the load resistance (R_{Li}) is much larger than the coil resistance (R_i), so overall system efficiency can be simplified as

$$PTE = \frac{\sum_{i=1}^{n} Z_{ri} \cdot \frac{R_{Li}}{R_{ri} + R_{Li}}}{R_t + \sum_{i=1}^{n} Z_{ri}} \approx \frac{1}{\frac{R_t}{\sum_{i=1}^{n} Z_{ri}} + 1} \tag{10}$$

It can be obviously seen that the overall efficiency can be improved by increasing the number of receivers. In other words, for a given voltage, the total output power will be enhanced by increasing the number of Rx coil.

According to coupling theory, the current for i_{th} RX coil can be given as

$$I_{ri} = \frac{-j\omega Mti}{(R_{Li} + R_i)(\sum_{i=1}^{n} Z_{Ri} + R_t)} VS \tag{11}$$

TABLE 2. Lumped element values of the proposed coils.

TX coil		RX_1 coil		RX_2 coil	
Parameter	Value	Parameter	Value	Parameter	Value
$R_t(\Omega)$	1.12	$R_1(\Omega)$	0.17	$R_2(\Omega)$	0.18
$L_t(\mu H)$	838.93	L_1	76.58	L_2	76.82
$C_t(nF)$	4.32	$C_1(nF)$	45.16	C_2	45.02
Working frequency		84.5kHz			

TABLE 3. Mutual inductance between the proposed coils.

D (cm)	$M_{t1}(\mu H)$	$M_{t2}(\mu H)$	$M_{12}(\mu H)$
20	3.31	3.30	0.26
25	1.82	1.81	0.06
30	1.15	1.15	0.05

The output power for i_{th} load can be calculated as

$$P_i = \frac{(\omega M_{ti})^2 VS^2}{(R_{Li} + R_i)^2 (\sum_{i=1}^{n} Z_{Ri} + Rt)^2} R_{Li} \tag{12}$$

Therefore, the power ratio of any two RX coils can be expressed as

$$\frac{P_i}{P_j} = \frac{PTE_i}{PTE_j} = \frac{M_{ti}^2 (R_j + R_{Lj})^2 R_{Li}}{M_{tj}^2 (R_i + R_{Li})^2 R_{Lj}} \tag{13}$$

It can be found from (8)-(13) that when the number of loads in the system changes, it affects the overall reflected impedance at the TX coil. More specifically, the current and output power of i_{th} RX coil will decrease when the number of RX coil increases. It can be obviously seen that each output power of the RX coil is very closely related to the mutual inductance between the RX coil and TX coil. The greater mutual inductance, namely the smaller distance, the more output power is distributed.

From the equations above, it can be seen obviously that the strength of coupling between the TX coil and each RX coil and load resistance are two key considerations for multiple pick-ups WPT systems. Here, a WPT system with two pick-ups is adopted as an example to illustrate the above rules. The example coil circuit parameters are given in Table 2. Compared to the air core coil, the resistance of the magnetic dipole coil is relatively large due to the existence of auxiliary resistance caused by the hysteresis loss of the ferrite. Note that the resistances of magnetic dipole coil are achieved in AC mode at the working frequency of 84.5 kHz. It should be mentioned that the mutual inductance between the TX coil and RX coil (M_{t1} and M_{t2}) is much larger than M_{12}, as listed in Table 3. Therefore, the mutual inductance of each RX coil can be neglected in the practical scenarios.

As shown in Fig. 21, the influences of the mutual inductances on PTE for two identical RX coils are discussed. It can be found that the values of optimal loads vary with the change of the distance between the transmitter and receiver. As the distance increases, the value of maximum load will decrease and tend to be close to the internal resistance of RX coil (R_i). Besides, PTE can stay high level when the load varies in a certain zone, especially in case when the value is larger than

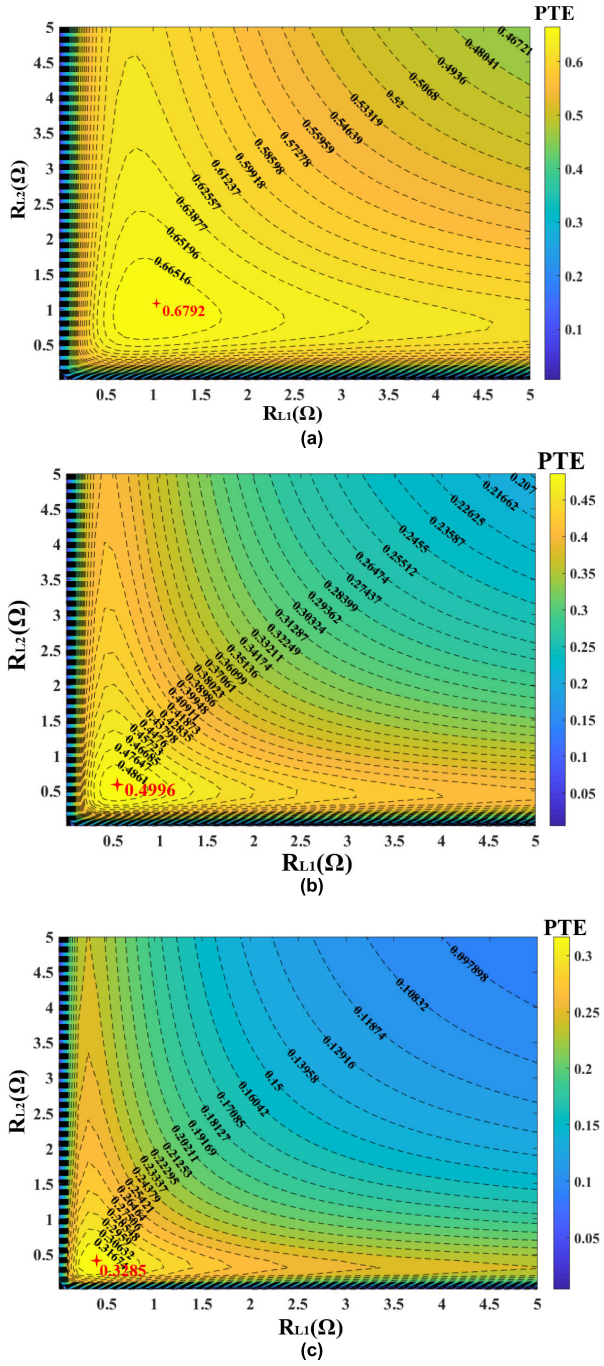

FIGURE 21. PTEs as a function of two load resistances. (a) D = 20cm. (b) D = 25cm. (c) D = 30cm.

the optimal load. In order to achieve high PTE in WPT system for multiple pickups, the load of RX coil needs to get closer to the optimal load and can be slightly higher than it.

IV. EXPERIMENTS AND RESULTS

Two groups of experiments are implemented to verify the proposed methodology. The first part of the experiment is performed to focus on the 3D omnidirectional characteristic of the novel cubic transmitter coil design. The second part of the experiment is carried out to analyze the transmission performances of multiple pick-ups. The proposed cubic TX coil in this paper consists of 12 magnetic dipole coils. For better winding of Litz wire and fabrication, the acrylic sheet with grooves is used. It can also reduce the parasitic capacitance between the wires and core effectively.

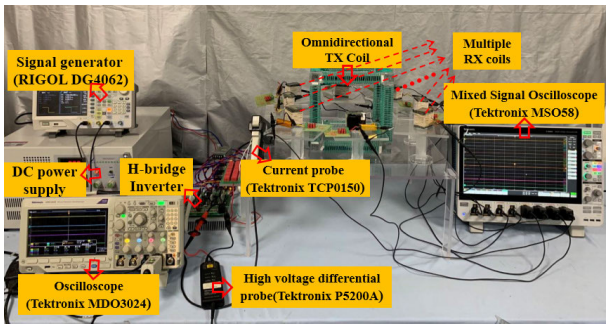

FIGURE 22. Experimental setup of the omnidirectional (or multiple RX coils) WPT system.

A. OMNIDIRECTIONAL TRANSMISSION

As shown in Fig. 22, an experimental setup is built to discuss the feasibility of the proposed omnidirectional WPT systems, which mainly consists of a power excitation (a DC source and an H-bridge DC/AC inverter), a resonance mechanism (the TX coil and RX coils), and load terminals. It is worth mentioning that mixed signal oscilloscope (Tektronix MSO58) has eight test channels, which is specially used to measure the voltage/current of multiple pick-ups. The key predefined circuit parameters are listed in Table 1. All parameters are measured by LCR METER (MICROTEST 6379) at AC mode. All the coils are fabricated by winding Litz wires over ferrite, which forms magnetic dipoles to improve the transfer efficiency and extend the transmission distance. Only one RX coil is used in this section to study the property of omnidirectional transmission.

Fig. 23 depicts that PTEs vary with the receiving angles at different transfer distances (at XOY orientation). The RX coil is placed in different positions and moves intermittently at 45 degree angle. The PTEs are basically the same when the RX coil is facing the TX coil or on the diagonal. However, the PTEs of the diagonal are slightly larger because of the greater mutual inductances. As the distance increases, the PTEs are decreased shapely due to the weak coupling. It can be seen obviously that the experimental results agree very well with calculated values. Further experiments show that the variation trends of three directions (XOY, YOZ and XOZ) are also consistent.

Fig. 24 shows PTEs at transmission distance of 20 cm and 30 cm. It can be seen that PTEs stay constant when input power ranges from 4 to 20W at given angle. It indicates that the core loss does not increase significantly when the input power goes up because the core does not reach saturation. The PTEs of the diagonal are also larger than these facing the TX coil at 20 cm. As the distance increases to around 30 cm, the PTEs tend to be consistent due to the homogeneous magnetic field at all receiving angles.

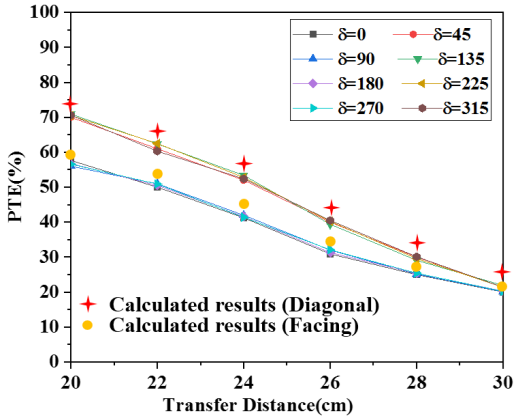

FIGURE 23. Magnetic field distributions for Rx coils of different dimensions.

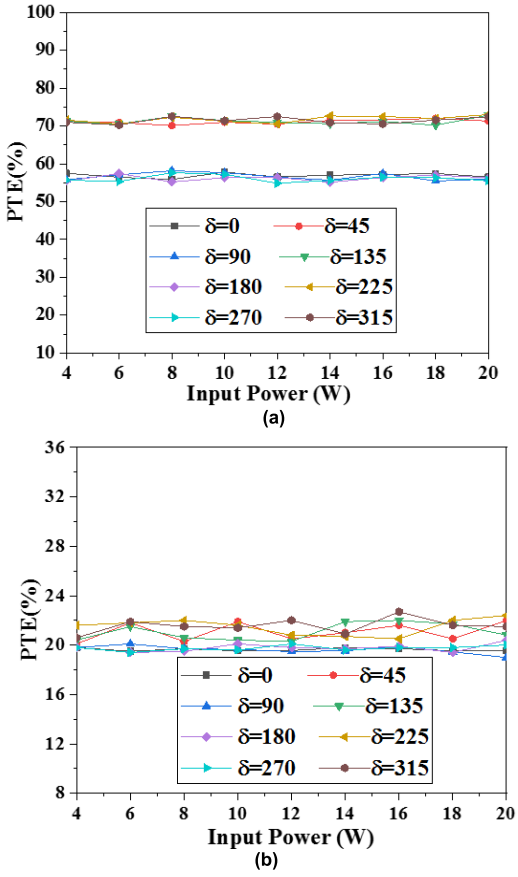

FIGURE 24. PTEs as a function of input power of transfer distance at (a) 20cm. (b) 30cm.

B. MULTIPLE PICKUPS

The experimental setup for the second part is depicted in Fig. 22. First, the impact of the existence of multiple RX coils on the TX coil inductance should be discussed. That is because the inductance of the magnetic dipole coil would be affected by the ambient environment indeed due to the introduction of the ferrite. Here, the worst-case scenario has been investigated to illustrate the effect of multiple RX coils on the inductance of TX coil, namely, when there are eight RX coils placed around TX coil, the inductance of TX coil

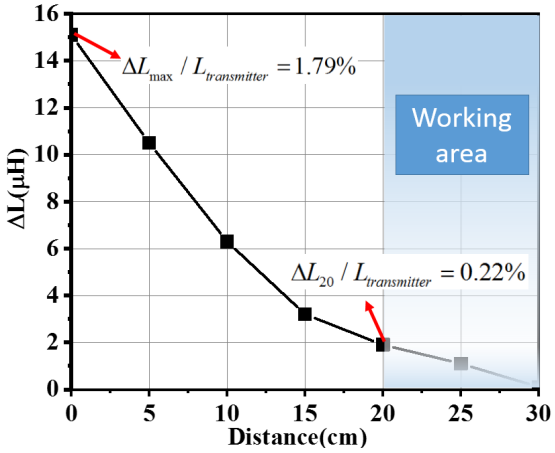

FIGURE 25. Increment of TX coil inductance for eight RX coils.

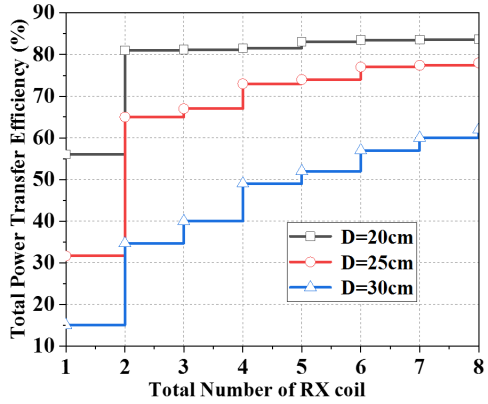

FIGURE 26. Total PTEs with identical RX coil at different transfer distance and numbers of RX coils.

changes with the distance (the distance between TX coil and each RX coil) has been analyzed. As shown in Fig. 25, ΔL denotes the inductance increment of the TX coil. It can been seen that the increment of the TX inductance is maximum when the distance between the eight RX coils and the TX coil is all zero simultaneously. The maximum normalized value of TX coil inductance (the ratio of the inductance increment and self-inductance of TX coil) is very tiny, about 1.79%. Moreover, the odds of this case are very small for the WPT systems, which aim to transmit energy over long distance wirelessly. As the distance increases, the increments decrease rapidly. It means the impact of the multiple RX coils on transmitter diminishes sharply. In addition, it has little effect on TX coil inductance when all RX coils are positioned in working distance analyzed in this paper (the distance between TX coil and each RX coil is over 20cm). Therefore, the influence of the existence of multiple RX coils on the TX coil inductance will not be considered.

Fig. 26 plots PTEs with different numbers of RX coils at the same transmission distance. The RMS value of the voltage for the load resistance of each RX coil can be obtained by the oscilloscope. Then the total output power for each RX coil can be calculated. Eventually, total PTEs for multiple receivers can be achieved by calculating the ratio of the total output power to the input power. The circuit parameters of

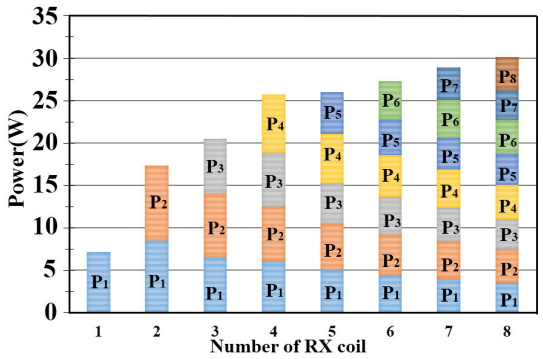

FIGURE 27. Power distribution for each RX coil at D = 30cm.

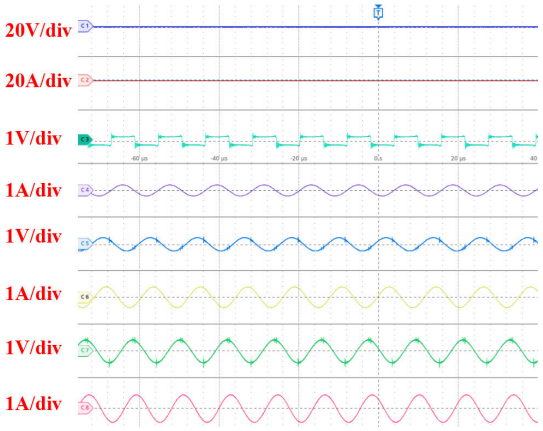

FIGURE 28. Measured steady-state waveforms with two RX coils. Ch1: Voltage of DC power supply. Ch2: Current of DC power supply. Ch3: Output voltage of H-bridge invert. Ch4: Output current of H-bridge invert. Ch5: Voltage of RX1 coil. Ch6: Current of RX1 coil. Ch7: Voltage of RX2 coil. Ch8: Current of RX2 coil.

each RX coil are basically the same. As the number of RX coil increases, the efficiency for existed load decreases a high magnitude, while the total efficiency will jump up. However, the upward trend will slow down as the number of RX coil continues to increase. Fig. 27 shows the power distribution among RX coils. The output power for each RX coil is basically uniformly distributed. According to Equation (8), as the number of load infinitely increases, the total PTE approaches

$$PTE_{n\to\infty} = \frac{R_{Li}}{R_i + R_{Li}} \tag{14}$$

Fig. 28 shows the voltage and current waveforms of input and output terminals for two RX coils. Each load resistances of two coil is 1Ω and the RMS of the output voltage is about 1.6 V. The input voltage for TX coil (Ch4) is almost in phase with the current (Ch5) (voltage is slightly ahead of current), which is to achieve soft-switch state for the inverter. The reactive power in the circuit is reduced largely to keep high conversion efficiency. The slight phase deviation of the two RX coils output waveforms is due to resonator fabrication and experimental errors and these errors are also within the allowed range. Fig. 29 shows the voltage and current waveforms of input and output terminals for four RX coils, which are arbitrarily positioned to verify the omnidirectional and free-positioning transmission performances. Similarly,

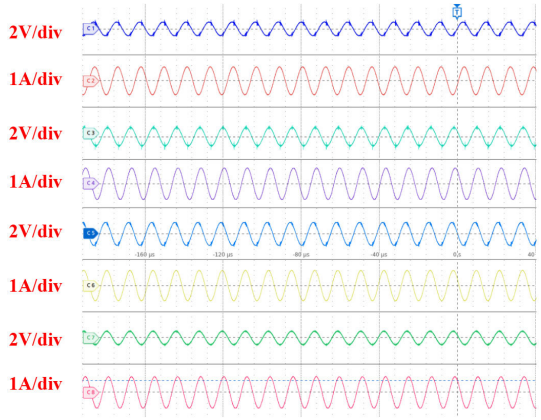

FIGURE 29. Measured steady-state waveforms with four RX coils. Ch1 and Ch2: Voltage and current of RX1 coil. Ch3 and Ch4: Voltage and current of RX2 coil. Ch5 and Ch6: Voltage and current of RX3 coil. Ch7 and Ch8: Voltage and current of RX4 coil.

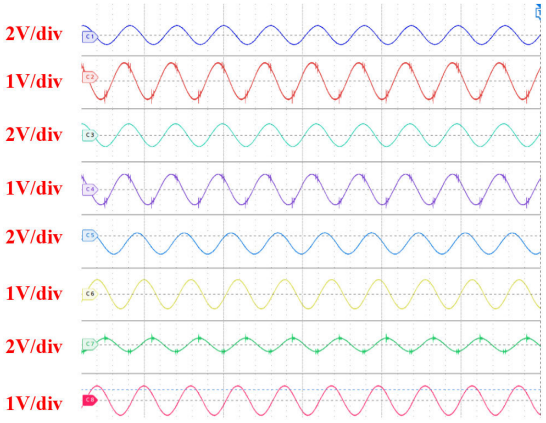

FIGURE 30. Measured steady-state waveforms with eight RX coils. Each channel measures voltage of one RX coil.

the output voltage is around 2V and output waveforms are also identical on the whole. As expected, the current and voltage received by the four receiving coils are basically the same phase and magnitude. Furtherly, the voltages of eight RX coils are measured, as shown in Fig. 30. It can be seen that slightly lower voltage at opposite TX coil compared to that at diagonal position is due to the tiny different of the mutual inductance. The RMS of each RX coil voltage is about 2V and the total output power can reach above 30W. For these three waveform diagrams, the output voltages and currents are essentially in phase and can be used for calculating the power dissipation of RX coils. The measured results show that the proposed coupling mechanism can effectively increase system stability for 3D omnidirectional and multiple-pickup WPT system in spite of the angular misalignment and the number of multiple load, which is also consistent with the theoretical analysis.

Table 4 compares the transfer performance of omnidirectional WPT systems in recent years. According to this table, the cubic transmitter based on magnetic dipole coil has a compatible great property and competitive advantage due to its flexibility.

TABLE 4. Reported omnidirectional WPT systems ('-' means not given).

Reference	Structure	WPT type	Resonant Frequency	Power	Efficiency	Load type
[4]	Three orthogonal square coils	3D full-range field orientation	19.59 kHz	13.7W	28.2%	1
[10]	Three orthogonal round coils	3D omnidirectional	-	1.07W	69.5%	1
[14]	Hollow metallic structure	Multimode Resonant Cavity	191.65 MHz	8W	20%-30%	10 LEDs
[15]	Cubic	2D omnidirectional	13.56 MHz	10W	~60%	1
[16]	Bowl-shaped transmitter	Free positioning and omnidirectional	6.78 MHz	2.5W	60%	1
[28]	Two decoupled receivers	Rotational insensitivity	252.6 kHz	664W	92.26%	1
This work	Cubic transmitter	Genuine 3D omnidirectional	84.5 kHz	30 W	60%	8 bulbs

V. CONCLUSION

This paper has presented and implemented a novel 3D omnidirectional and multiple-pickup WPT systems to realize real 3D high DoF and multiple loads. The structure of TX coil is designed using 12 magnetic dipole coils with particular current directions. From the calculated, simulated and experimental results, it has been validated that the cubic transmitter has the ability of 3D omnidirectional and multi-load transmission performance. In addition, with respect to the number of RX coil, the efficiency of the proposed system can effectively jump up and the output power can be evenly distributed. Compared with the traditional WPT systems with air coil, the proposed system can achieve efficiency above 60% under multiple pick-ups and the total output power can reach over 30 W, which meets most of the lower power requirements. The proposed WPT system shows a great promising prospect in numerous industrial applications.

REFERENCES

[1] A. Kurs, A. Karalis, R. Moffatt, J. D. Joannopoulos, P. Fisher, and M. Soljačić, "Wireless power transfer via strongly coupled magnetic resonances," *Science*, vol. 317, no. 5834, pp. 83–86, Jul. 2007.

[2] J. P. K. Sampath, A. Alphones, and D. M. Vilathgamuwa, "Figure of merit for the optimization of wireless power transfer system against misalignment tolerance," *IEEE Trans. Power Electron.*, vol. 32, no. 6, pp. 4359–4369, Jun. 2017.

[3] H. Han, Z. Mao, Q. Zhu, M. Su, and A. P. Hu, "A 3D wireless charging cylinder with stable rotating magnetic field for multi-load application," *IEEE Access*, vol. 7, pp. 35981–35997, 2019.

[4] Q. Zhu, M. Su, Y. Sun, W. Tang, and A. P. Hu, "Field orientation based on current amplitude and phase angle control for wireless power transfer," *IEEE Trans. Ind. Electron.*, vol. 65, no. 6, pp. 4758–4770, Jun. 2018.

[5] W. Tang, Q. Zhu, J. Yang, D. Song, M. Su, and R. Zou, "Simultaneous 3-D wireless power transfer to multiple moving devices with different power demands," *IEEE Trans. Power Electron.*, vol. 35, no. 5, pp. 4533–4546, May 2020.

[6] Z. Ye, Y. Sun, X. Liu, P. Wang, C. Tang, and H. Tian, "Power transfer efficiency analysis for omnidirectional wireless power transfer system using three-phase-shifted drive," *Energies*, vol. 11, no. 8, p. 2159, Aug. 2018.

[7] W. M. Ng, C. Zhang, D. Lin, and S. Y. Ron Hui, "Two- and three-dimensional omnidirectional wireless power transfer," *IEEE Trans. Power Electron.*, vol. 29, no. 9, pp. 4470–4474, Sep. 2014.

[8] D. Lin, C. Zhang, and S. Y. R. Hui, "Mathematical analysis of omnidirectional wireless power transfer—Part-I: Two-dimensional systems," *IEEE Trans. Power Electron.*, vol. 32, no. 1, pp. 625–633, Jan. 2017.

[9] Z. Zhang and B. Zhang, "Angular-misalignment insensitive omnidirectional wireless power transfer," *IEEE Trans. Ind. Electron.*, vol. 67, no. 4, pp. 2755–2764, Apr. 2020.

[10] C. Zhang, D. Lin, and S. Y. Hui, "Basic control principles of omnidirectional wireless power transfer," *IEEE Trans. Power Electron.*, vol. 31, no. 7, pp. 5215–5227, Jul. 2016.

[11] B.-J. Che, G.-H. Yang, F.-Y. Meng, K. Zhang, J.-H. Fu, Q. Wu, and L. Sun, "Omnidirectional non-radiative wireless power transfer with rotating magnetic field and efficiency improvement by metamaterial," *Appl. Phys. A, Solids Surf.*, vol. 116, no. 4, pp. 1579–1586, Sep. 2014.

[12] Z. Dai, Z. Fang, H. Huang, Y. He, and J. Wang, "Selective omnidirectional magnetic resonant coupling wireless power transfer with multiple-receiver system," *IEEE Access*, vol. 6, pp. 19287–19294, 2018.

[13] B.-J. Che, F.-Y. Meng, and Q. Wu, "An omnidirectional wireless power transmission system with controllable magnetic field distribution," in *Proc. IEEE Int. Workshop Electromagn., Appl. Student Innov. Competition (iWEM)*, May 2016, pp. 1–3.

[14] M. J. Chabalko and A. P. Sample, "Three-dimensional charging via multimode resonant cavity enabled wireless power transfer," *IEEE Trans. Power Electron.*, vol. 30, no. 11, pp. 6163–6173, Nov. 2015.

[15] N. Ha-Van and C. Seo, "Analytical and experimental investigations of omnidirectional wireless power transfer using a cubic transmitter," *IEEE Trans. Ind. Electron.*, vol. 65, no. 2, pp. 1358–1366, Feb. 2018.

[16] J. Feng, Q. Li, F. C. Lee, and M. Fu, "Transmitter coils design for free-positioning omnidirectional wireless power transfer system," *IEEE Trans. Ind. Informat.*, vol. 15, no. 8, pp. 4656–4664, Aug. 2019.

[17] J. Feng, Q. Li, and F. C. Lee, "Omnidirecitional wireless power transfer for portable devices," in *Proc. IEEE Appl. Power Electron. Conf. Expo. (APEC)*, Mar. 2017, pp. 1675–1681.

[18] R.-C. Kuo, P. Riehl, and J. Lin, "3-D wireless charging system with flexible receiver coil alignment," in *Proc. IEEE Wireless Power Transf. Conf. (WPTC)*, May 2016, pp. 1–4.

[19] M. Wang, J. Feng, Y. Shi, and M. Shen, "Demagnetization weakening and magnetic field concentration with ferrite core characterization for efficient wireless power transfer," *IEEE Trans. Ind. Electron.*, vol. 66, no. 3, pp. 1842–1851, Mar. 2019.

[20] M. Budhia, G. Covic, and J. Boys, "A new IPT magnetic coupler for electric vehicle charging systems," in *Proc. IECON 36th Annu. Conf. IEEE Ind. Electron. Soc.*, Nov. 2010, pp. 2487–2492.

[21] M. Mohammad, S. Kwak, and S. Choi, "Core design for better misalignment tolerance and higher range of wireless charging for HEV," in *Proc. IEEE Appl. Power Electron. Conf. Expo. (APEC)*, Mar. 2016, pp. 1748–1755.

[22] B. H. Choi, V. X. Thai, E. S. Lee, J. H. Kim, and C. T. Rim, "Dipole-coil-based wide-range inductive power transfer systems for wireless sensors," *IEEE Trans. Ind. Electron.*, vol. 63, no. 5, pp. 3158–3167, May 2016.

[23] C. Park, S. Lee, G.-H. Cho, and C. T. Rim, "Innovative 5-m-off-distance inductive power transfer systems with optimally shaped dipole coils," *IEEE Trans. Power Electron.*, vol. 30, no. 2, pp. 817–827, Feb. 2015.

[24] B. H. Choi, E. S. Lee, Y. H. Sohn, G. C. Jang, and C. T. Rim, "Six degrees of freedom mobile inductive power transfer by crossed dipole Tx and Rx coils," *IEEE Trans. Power Electron.*, vol. 31, no. 4, pp. 3252–3272, Apr. 2016.

[25] E. S. Lee, J. S. Choi, H. S. Son, S. H. Han, and C. T. Rim, "Six degrees of freedom wide-range ubiquitous IPT for IoT by DQ magnetic field," *IEEE Trans. Power Electron.*, vol. 32, no. 11, pp. 8258–8276, Nov. 2017.

[26] X. Dai, L. Li, X. Yu, Y. Li, and Y. Sun, "A novel multi-degree freedom power pickup mechanism for inductively coupled power transfer system," *IEEE Trans. Magn.*, vol. 53, no. 5, pp. 1–7, May 2017.

[27] G. Liu, B. Zhang, W. Xiao, D. Qiu, Y. Chen, and J. Guan, "Omnidirectional wireless power transfer system based on rotary transmitting coil for household appliances," *Energies*, vol. 11, no. 4, p. 878, Apr. 2018.

[28] Z. Yan, B. Song, Y. Zhang, K. Zhang, Z. Mao, and Y. Hu, "A rotation-free wireless power transfer system with stable output power and efficiency for autonomous underwater vehicles," *IEEE Trans. Power Electron.*, vol. 34, no. 5, pp. 4005–4008, May 2019.

[29] M. Fu, T. Zhang, C. Ma, and X. Zhu, "Efficiency and optimal loads analysis for multiple-receiver wireless power transfer systems," *IEEE Trans. Microw. Theory Techn.*, vol. 63, no. 3, pp. 801–812, Mar. 2015.

[30] D. Ahn and S. Hong, "Effect of coupling between multiple transmitters or multiple receivers on wireless power transfer," *IEEE Trans. Ind. Electron.*, vol. 60, no. 7, pp. 2602–2613, Jul. 2013.
[31] Z. Zhang and H. Pang, "Continuously adjustable capacitor for multiple-pickup wireless power transfer under single-power-induced energy field," *IEEE Trans. Ind. Electron.*, vol. 67, no. 8, pp. 6418–6427, Aug. 2020.
[32] D. Ahn, S.-M. Kim, S.-W. Kim, J.-I. Moon, and I.-K. Cho, "Wireless power transfer receiver with adjustable coil output voltage for multiple receivers application," *IEEE Trans. Ind. Electron.*, vol. 66, no. 5, pp. 4003–4012, May 2019.
[33] S. Wang, Z. Hu, C. Rong, C. Lu, J. Chen, and M. Liu, "Planar multiple-antiparallel square transmitter for position-insensitive wireless power transfer," *IEEE Antennas Wireless Propag. Lett.*, vol. 17, no. 2, pp. 188–192, Feb. 2018.
[34] S. Babic, F. Sirois, C. Akyel, G. Lemarquand, V. Lemarquand, and R. Ravaud, "New formulas for mutual inductance and axial magnetic forcebetween a thin wall solenoid and a thick circular coil of rectangular crosssection," *IEEE Trans. Magn.*, vol. 47, no. 8, pp. 2034–2044, Aug. 2011.
[35] L. Ke, G.-Z. Yan, S. Yan, Z.-W. Wang, and D.-S. Liu, "Coupling analysis of transcutaneous energy transfer coils with planar sandwich structure for a novel artificial anal sphincter," *J. Zhejiang Univ. Sci. C*, vol. 15, no. 11, pp. 1021–1034, Nov. 2014.

CANCAN RONG was born in China, in 1991. He received the B.E. degree in electrical engineering and automation from Jiangsu Normal University. He is currently pursuing the Ph.D. degree with the State Key Laboratory of Advanced Electromagnetic Engineering and Technology, Huazhong University of Science and Technology, Wuhan, China. His current research interests include wireless power transfer and metamaterials.

XIANGRUI HE was born in Jiangxi, China, in 1999. He is currently pursuing the B.E. degree with the School of Electrical and Electronic Engineering, Huazhong University of Science and Technology, Wuhan, China. His current research interests include wireless power transfer and magnetic materials.

MINGHAI LIU received the Ph.D. degree in physics from the University of Science and Technology of China, Hefei, China, in 1997. From 1997 to 1999, he was a Postdoctoral Fellow with the Institute of Plasma Physics, Chinese Academy of Sciences, Hefei. From 2002 to 2004, he was a Visiting Scholar with Nagoya University, Nagoya, Japan. Since 2000, he has been with the Huazhong University of Science and Technology, Wuhan, China, where he is currently a Professor with the State Key Laboratory of Advanced Electromagnetic Engineering and Technology. His research interests mainly include metamaterials and wireless power transfer systems.

YUYING WANG was born in Qixia, Shangdong, China, in 1993. She received the B.E. degree in physics from Zaozhuang University, in 2016, and the M.S. degree in physics from Qufu Normal University, in 2019. She is currently pursuing the Ph.D. degree with Xiamen University. Her research interests include surface plasmon, nanophotonics, and biosensor detection.

XIAOBO LIU was born in China, in 1996. He received the B.Eng. degree in electrical engineering and automation from Ningxia University, Ningxia, China, in 2019. He is currently pursuing the M.E. degree with the State Key Laboratory of Advanced Electromagnetic Engineering and Technology, School of Electrical and Electronic Engineering, Huazhong University of Science and Technology, Wuhan, China. His current research interest includes design and analysis of wireless power transfer systems.

CONGHUI LU was born in China, in 1994. She received the B.S. degree in physics from Zaozhuang University and the M.E. degree from the School of Physics, Huazhong University of Science and Technology, Wuhan, in 2019. She is currently pursuing the Ph.D. degree with the State Key Laboratory of Advanced Electromagnetic Engineering and Technology, Huazhong University of Science and Technology, Wuhan. Her current research interest includes wireless power transfer systems.

YINGQIN ZENG was born in China, in 1996. She received the B.E. degree in electrical engineering and automation from the Hebei University of Technology. She is currently pursuing the master's degree with the State Key Laboratory of Advanced Electromagnetic Engineering and Technology, School of Electrical and Electronic Engineering, Huazhong University of Science and Technology, Wuhan, China. Her current research interest includes wireless power transfer systems using metamaterials.

RENZHE LIU received the B.E. degree in electrical and electronic engineering from the Huazhong University of Science and Technology (HUST), Wuhan, China, in 2017, where he is currently pursuing the M.E. degree with the School of Electrical and Electronic Engineering. His current research interest includes wireless power transfer.